Studies on the First DSC Endotherm of Polyurethane Hard Segment Based on 4,4′-Diphenylmethane Diisocyanate and 1,4-Butanediol

Teng Ko Chen,* Tien Shou Shieh, and Jia Yeong Chui

Department of Chemical Engineering, National Central University, Chung-li, Taiwan 32054, Republic of China

Received June 23, 1997; Revised Manuscript Received October 13, 1997

ABSTRACT: The first high-temperature endotherm (T_1) of polyurethane hard segment based on 4,4′-diphenylmethane diisocyanate (MDI) and 1,4-butanediol (BD) was studied by differential scanning calorimetry (DSC). The materials contain 69% (w/w) of MDI and BD as the hard segment and hydroxyl-terminated *cis*-polybutadiene with number average molecular weights of 1650 and 2300, respectively, as the soft segment. The hard segment and the soft segment of these polyurethanes appear to be very completely phase-separated, giving rise to very simplified material structures for this study. Samples under melt-quenched condition gave rise to a highly amorphous phase for the hard phase and a distinct hard-segment glass transition behavior, which enabled us to study the T_1 behavior in relation to the amorphous hard-segment T_g (T_{gh}). Upon annealing below the T_{gh} of the pure amorphous hard phases, both the T_1 temperature and magnitude of the T_1 endotherm increased linearly with the increase in logarithmic annealing time (log t_a). On the other hand, if the polyurethane were first annealed to form multiple endotherms at noncrystalline T_2 region, the annealing above the previous T_{gh} gave rise to a T_1 which also increased linearly in temperature with the increase in log t_a. These phenomena are typical of enthalpy relaxations resulting from the physical aging of the amorphous hard segment. Thus, we suggest the long-term confusing nature of T_1 is due to an enthalpy relaxation of the amorphous hard segment. On the other hand, we also suggest that T_2, which was previously associated with a long-range order of unspecified nature, would disturb the amorphous hard segment and cause a rise in the T_g in different degrees to a higher temperature near T_2.

Introduction

Segmented polyurethane elastomers are linear block copolymers of −(HS)$_n$− type (H, hard segment; S, soft segment), whose versatile physical properties are generally attributed to their microphase-separated structure. The hard-segment microdomains act as thermally labile physical cross-linking sites as well as fillers for the rubbery soft-segment matrix. A large number of previous investigations had reported on the characterization of this microdomain structure using a variety of experimental techniques.

One important aspect of the hard-segment-phase behavior that remains uncertain is the morphological origin of the apparent multiple melting endotherms observed in the DSC study of the polyurethane hard-segment phase. The first low-temperature endotherms (designated as T_1) observed at some 20−30 °C above the annealing temperature had been generally ascribed to a short-range order of unknown nature.[1−3] An intermediate endotherm (T_2) observed between 120−200 °C was attributed to a hard segment long-range order[1−3] of unspecified nature or to the onset of the microphase mixing[4,5] of the hard and soft microphases. Finally, an endotherm (T_3) occurring above 200 °C is typically attributed to the melting of the hard segment microcrystalline region.[1−3] This present article describes a complete study on the fundamental nature of the T_1 behavior.

Seymour and Cooper[1] indicated that T_1 can be improved by annealing, resulting in an increase of the T_1 temperature with increasing annealing temperature. They proposed that T_1 was a result from the melting of a short-range order of unknown nature. Later, Cooper et al.[2] also found that T_1 endotherm was absent in the DSC thermogram, when taken immediately after quenching to room temperature from the annealing temperature at 120, 150, and 170 °C, but it reappeared some time after quenching, and, at a long time, shifted to some higher temperature and grew larger in size. They indicated that this later phenomenon was an achievement of better short-range order. Cooper et al.[3] further indicated that T_1 also had appeared in pure hard segment materials. They consequently suggested that the induced ordering would occur within the hard microdomain rather than in the interphase between domains.

Alternatively, Koberstein et al.[6] in their studies on a series of compression-molded polyurethane found a possible glass transition process that occurs in the region 50−90 °C. The transition was manifested as a small peak or as a change in the slope of the DSC baseline. Koberstein et al. studied the shape of this transition at different scan rates and compared the results with the catastrophic softenings from the thermal mechanical analysis (TMA). They propose that the DSC transitions in the 50−90 °C region are reflective of an apparent hard microdomain T_g process. This was in contrast to Cooper's previous studies.[1−3] More recently, Koberstein et al.,[7] in their study on conventional polyether polyurethanes, suggested another reason for the T_1 behavior. They indicated that the temperature dependence of the T_1 endotherm may be explained by solubility effects[8] embodied in the microdomain model developed by Koberstein and Stein.[9] That is, there is a critical hard segment sequence length, N_D, below which hard segments dissolved within the soft microphase. At low annealing temperatures (i.e. N_D is low), short and

* To whom correspondence should be addressed.

S0024-9297(97)00913-3 CCC: $15.00
Published on Web 01/31/1998

long hard segments separate from the soft microphase. Because of the limited mobility of long hard segments at a low annealing temperature, only short ones can align to form ordered structures. As the annealing temperature increases, the shorter hard segments become soluble in the soft microphases (N_D increases), and the ordering process is due to progressively longer hard segments. Therefore, T_1 increases with annealing temperature until it disappears at a higher annealing temperature.

From the above discussion, it is apparent that fundamental nature of the T_1 endotherm may be still obscure. However, if we accepted Koberstein's hard segment T_g from TMA study[6] and compare it with Cooper's T_1 phenomenon,[1−3] we find that they both appeared approximately at the same temperature range. Thus, we suspect that T_1 would very likely appear in the vicinity of the hard-segment T_g (T_{gh}). On the basis of this expectation, we further suspect that T_1 endotherm might be a phenomenon known as enthalpy relaxation resulting from physical aging of the amorphous hard segment.

Recently some of our novel polyurethane[10,11] based on MDI and BD as the hard segment and hydroxyl terminated *cis*-polyurethane (*cis*-HTPB) as the soft segment have shown a highly amorphous hard-segment phase and a clear amorphous hard-segment glass transition behavior. These polyurethanes enable us to study the T_1 behavior in relation to the hard-segment glass transition by controlling the aging process. The fundamental nature of the T_1 behavior is elucidated in this study.

Experimental Section

Segmented polyurethanes of various hard-segment content and of various soft-segment molecular weight were used in this study. The hard segments consist of 4,4′-diphenylmethane diisocyanate (MDI; T.C.I. Co.) and 1,4-butanediol (BD; Aldrich). The soft segments are hydroxyl terminated *cis*-polybutadiene (*cis*-HTPB; 96% cis structure). Functionality and molecular weight distribution of the *cis*-HTPB's approximately equal 2. A partial detail for the synthesis and characterization of *cis*-HTPB was given in our recent paper,[10] The complete detail was given elsewhere.[11] The *cis*-HTPB-based polyurethanes were prepared in a mixed solvent system of tetrahydrofuran (THF) and *N*,*N*′-dimethylacetamide (DMAc) at 1:1 (v/v). The *cis*-HTPB solution, containing 0.15% stannous octoate as catalyst, was added to the stirred MDI solution under dry nitrogen at 60−70 °C. After 1.5 h, a required amount of chain extender solution (5% w/v) was added dropwise over 30−35 min. Chain extension with stoichiometric amounts of butanediol required 12 h. The total amount of reactants in the mixed solution was around 10% (w/v). The mixed solution was clear throughout the reaction. Following the reaction, the polyurethane was precipitated from a large amount of water and dried at 50 °C in a vacuum. All of the polyurethanes' yields exceed 97%. Sample code is expressed as PU*xxxx-yy*, where *xxxx* denotes the soft segment molecular weight, and *yy* denotes the hard segment content. For instance, a polyurethane prepared from *cis*-HTPB at a molecular weight of 2300 and hard segment content (MDI + BD) of 35% (w/w) was designated as PU2300-35.

The polymer samples were prepared by casting the solution of 10% polyurethane in DMAc on a Teflon mold, followed by drying in air at 50 °C for 3 days and by vacuuming for 7 days at 60 °C. The films were stored in a desiccator under room temperature for at least 7 days before any DSC analysis. The films were transparent to visible light.

The DSC measurements at above ambient temperature were conducted using a Perkin-Elmer DSC-7 with an ice−water cooler in a nitrogen atmosphere. Indium was used to calibrate the temperature and heat of fusion. The weight of specimens was roughly 10 mg. The specimens were placed in aluminum pans and dried in a vacuum at room temperature for 1 day before performing the DSC experiments. All specimens were first heated to 240 °C and held at this temperature for 1 min to remove the thermal history. These samples were referred to as the melt-quenched samples because they were subsequently quenched to another annealing temperature and kept there for a fixed time period. The specimen after further annealing was quenched to 30 °C and subsequently scanned to 240 °C at a heating rate of 20 °C/min for DSC measurements. The magnitude of enthalpy relaxation resulting from annealing was calculated from the neat area obtained by subtracting the DSC thermogram of an unaged sample from that of an aged one. This is the method generally taken in the literature.[12−14] The peak position was also measured by the DSC-7 software, using the vertical cursors to locate the peak position. All the endothermic ΔH values have been corrected for their hard segment content.

The subambient DSC experiments were carried out with a liquid nitrogen cooler in a helium atmosphere. Both cyclohexane and indium were used to calibrate the temperature and heat of fusion. The thermal treatments of the melt-quenched samples were the same as those in the previous DSC study. After holding at 240 °C for 1 min, the sample were then quenched to −130 °C at a rate of 320 °C/min and kept at this temperature until thermal equilibrium was reached. The thermograms of the samples were subsequently measured at a heat rate of 20 °C/min from −120 °C to 230 °C.

Samples under annealing for more than 24 h were conducted inside a test tube under nitrogen atmosphere. The test tube was deeply immersed in a constant-temperature bath for a predescribed time.

Wide-angle X-ray scattering (WAXS) profile of the sample was collected at room temperature with a Siemens D500 diffractometer in transmission mode. The X-ray beam was nickel-filtered Cu Kα radiation ($\lambda = 0.1542$ nm) from a sealed tube operated at a voltage of 40 kV and a current of 30 mA. Data were obtained from 10 to 35° at a scan rate of 1.2°/min. Intensity recorded as a counting rate was plotted as a function of angle (2θ) on a strip-chart recorder.

Results and Discussion

Figure 1 shows the DSC thermograms for all the melt-quenched polyurethanes. The soft segment glass transition data are summarized in Table 1. For each series of polyurethanes of the same soft segment molecular weight, the soft phase T_g (T_gs) and the breadth of the glass transition (ΔBs) remain constant while the hard segment molecular weight changes for an order of magnitude. These phenomena are generally accredited to block's complete phase separation.[15,16] Furthermore, the PU1000-20 sample is quite unique, since it has only one MDI unit ($\bar{M}_{nh} = 250$) between the shortest soft segment ($\bar{M}_{ns} = 1000$). However, its T_gs and ΔBs are the same as those of other PU1000-*yy* samples. This datum indicates that the domain interfacial thickness may be much less than one MDI unit and decidedly strengthens the surmise that phase separation has been completed at the soft segment glass transition temperature.

After careful examination in Figure 1, we found that the melt-quenched polyurethanes with long soft segment and long hard segment, i.e., PU1650-69 and PU2300-69 samples, may show hard segment glass transition behavior at around 80 °C, which was first followed by a reordering exotherm and, then, immediately after the exotherm by a destructive endotherm for the newly formed ordered structure. To ensure that the transitions at around 80 °C were truly a T_g behavior, we had these melt-quenched PU1650-69

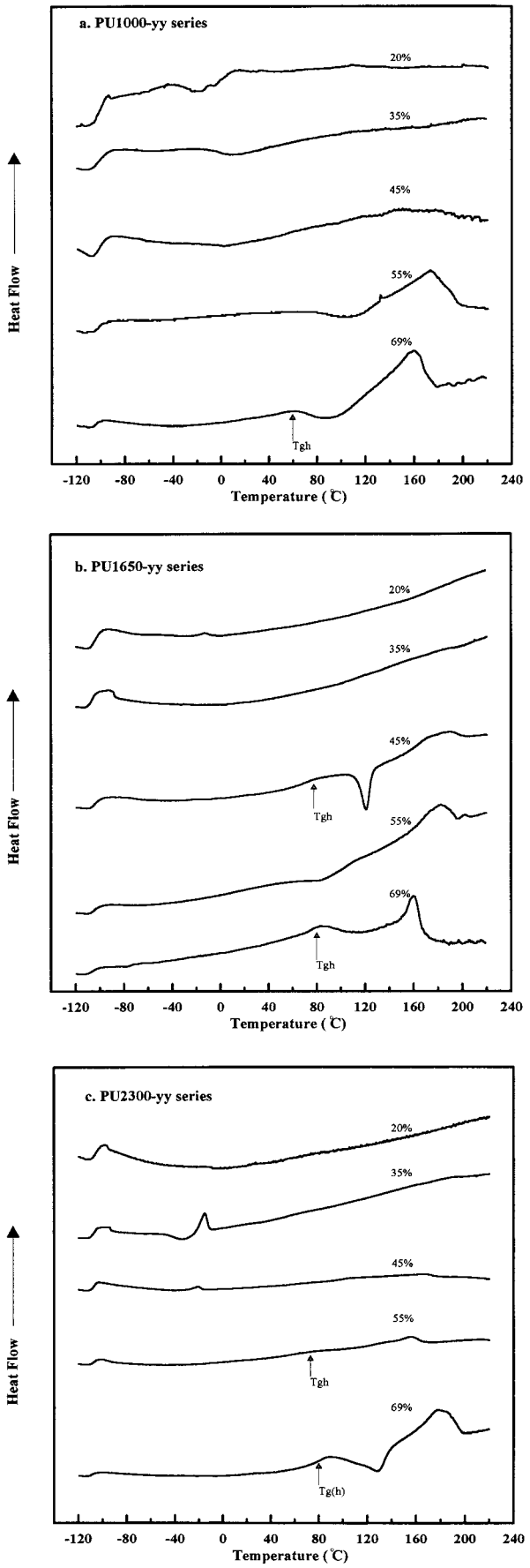

Figure 1. DSC thermograms for all the melt-quenched polyurethanes: (a) PU1000-*yy* series; (b) PU1650-*yy* series; (c) PU2300-*yy* series. *yy*% on each thermogram indicates hard segment content (wt %).

Table 1. Glass Transition Behaviors of the Polyurethane Soft Segments

sample	hard-segment molecular weight[a] $\bar{M}_{nh}$	glass transition behaviors[b] T_{gs} (°C)	ΔB (°C)
cis-HTPB1000		−109	6
PU1000-20	250	−102	10
PU1000-35	538	−103	11
PU1000-45	818	−103	11
PU1000-55	1222	−102	10
PU1000-69	2225	−104	11
cis-HTPB1650		−109	6
PU1650-20	413	−106	8
PU1650-35	888	−107	8
PU1650-45	1350	−106	8
PU1650-55	2017	−106	9
PU1650-69	3673	−107	9
cis-HTPB2300		−110	6
PU2300-20	575	−106	7
PU2300-35	1238	−108	6
PU2300-45	1882	−108	6
PU2300-55	2811	−108	7
PU2300-69	5119	−107	7

[a] The hard segmental number average molecular weight was calculated by the method[33] of $\bar{M}_{nh} = \bar{M}_{ns}(100\% - S_c)/S_c$, where $\bar{M}_{nh}$ is the hard segment number average molecular weight, $\bar{M}_{ns}$ is the soft segment number average weight, and S_c is the soft segment content (wt %). [b] T_{gs} and ΔB indicate the soft segment glass transition temperature and the breadth of the glass transition, respectively.

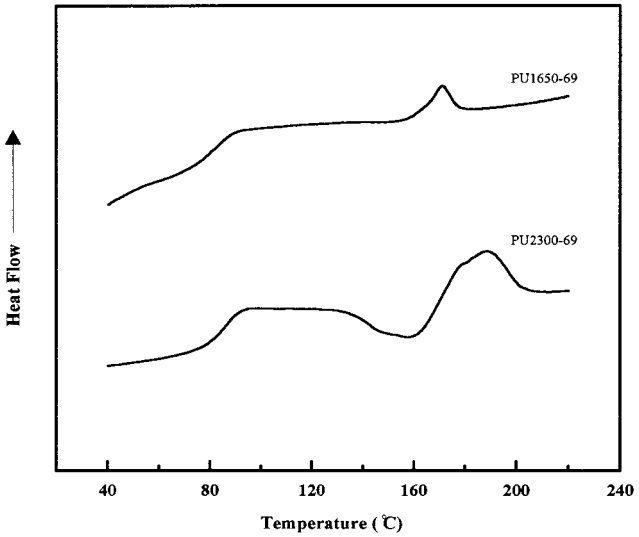

Figure 2. DSC thermograms for the melt-quenched PU1650-69 and PU2300-69 samples, which were further annealing at 175 °C for 1 h and for twenty minutes, respectively.

and PU2300-69 samples further annealed at 175 °C for 1 h and for 20 min, respectively, and then quenched to the room temperature for another DSC run (Figure 2). We obtained much clearer T_{gh} values at around 80 °C for these samples. The reason that the second annealing gives rise to a much less reordering exotherm has not been discussed in the literature. However, we suggest that it might relate to the morphological change of the hard-segment phase, which was annealed at different temperatures above T_{gh}.

On Figure 1, it is found that only the sample with 69% (w/w) hard segment can show a clear T_{gh} (i.e. one with a large heat capacity change). This is because the hard segment at this high content may constitute a continuous phase and the hard segment's segmental motion suffers a much lower entropy restriction effect,[17] which would, otherwise, lower the ΔC_{ph} value.

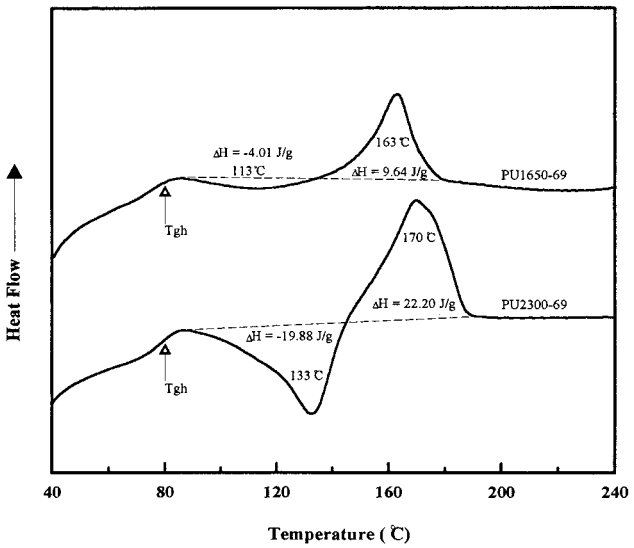

Figure 3. DSC thermograms for the melt-quenched PU1650-60 and PU2300-69 samples, measuring only at above room temperature.

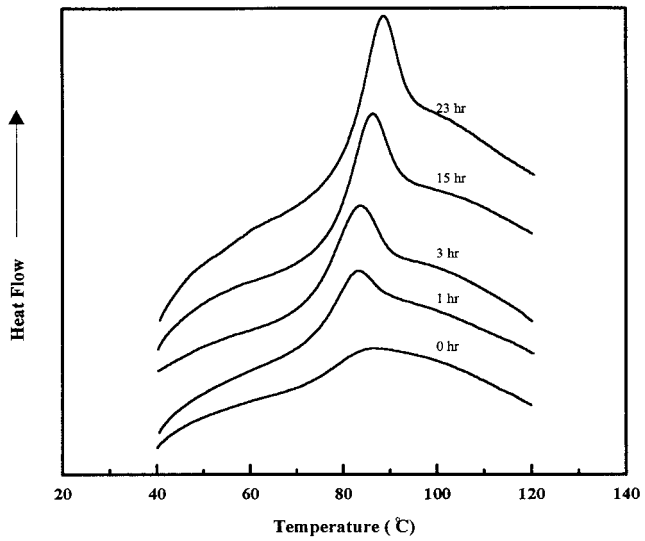

Figure 4. DSC thermograms of the melt-quenched PU2300-69 samples after further annealing at 60 °C for different time period.

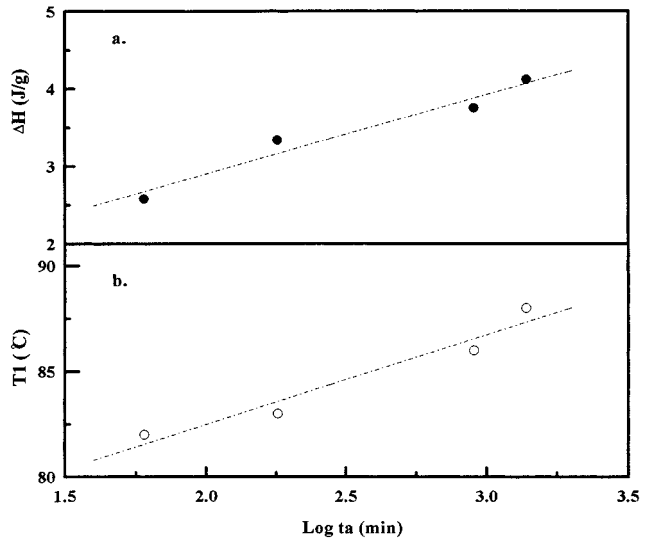

Figure 5. (a) Relationship of the endothermic magnitude, ΔH, with respect to the logarithm of the annealing time, t_a. (b) Relationship of the endothermic peak position, T_1, with respective to the logarithm of the annealing time. Both a and b are results from the DSC thermograms in Figure 4.

Careful examination on the previous DSC thermograms of both the PU1650-*yy* and the PU2300-*yy* series in parts b and c of Figure 1, respectively, we find that the baselines between the soft segment T_g at around −110 °C and the hard segment T_g at around 80 °C are all very level except for some very small peaks for the soft segments crystallizing exothermically and melting endothermically appearing between −60 and −10 °C for the PU2300-35 and the PU2300-45 samples (details on the study of the crystallization behavior in relation to the hard-segment morphology will be published in a separate paper[18]). Thus, we may assume that the complete phase-separated morphology at the soft-segment glass transition temperature will be retained up to the hard-segment glass transition temperature. Nevertheless, due to the shift of the DSC baseline, which may be very unexpected, some very broad thermal transitions may not be easily discernible in the DSC thermograms. To ensure that the samples under this study are completely separated at their hard-segment glass transition temperature, samples with higher hard segment molecular weights in both the PU1650-*yy* and PU2300-*yy* series could be taken with more confidence because the degree of phase separation always increases with increasing segmental molecular weight. From all these consideration, it is reasonable to assume that both PU1650-69 and PU2300-69 would retain their complete phase-separated morphology from the temperature of their soft-segment T_g up to the temperature of their hard-segment T_g.

Figure 3 enlarges the DSC thermograms for the melt-quenched PU1650-69 and PU2300-69 samples, but they are measured only at above room temperature. The glass transition temperature, the exotherm, and the endotherm are all similar to those in the complete thermograms measuring from −120 °C. After quantitative calculation, PU1650-69 sample exhibits an exotherm of $\Delta H = -4.01$ J/g with a peak minimum at 113 °C. This exotherm was further followed by an endotherm of $\Delta H = 9.64$ J/g with a peak maximum at 163 °C. All the ΔH's have been corrected for their hard-segment content. It is reasonable that enough segmental motion for the hard-segment reordering can only occur at above the hard-segment glass transition temperature, and this ordered structure can be further destroyed at a higher temperature. However, the absolute enthalpy change is more for the endotherm, indicating there is a probability of hard/soft segment dissolution at around 163 °C. However, since this extra endothermic enthalpy change is very small ($\Delta H = 5.63$ J/g) and the endothermic peak is very narrow, it is unlikely that a hard/soft segment dissolution would appear in this PU1650-69 sample, which has a broad hard segment molecular weight distribution. In a latter discussion in Figure 16, we will further indicate that complete phase separation can be retained up to 230 °C for the PU1650-69 sample. On the basis of our current understanding, the extra endothermic enthalpy at around 163 °C may result from a destruction of some long-range order formed during the sample's melt-quenched process. Furthermore, PU2300-69 sample behaves similar to the PU1650-69 sample in Figure 3. Since the PU2300-69 sample has higher hard-segment and higher soft-segment molecular weights, the sample

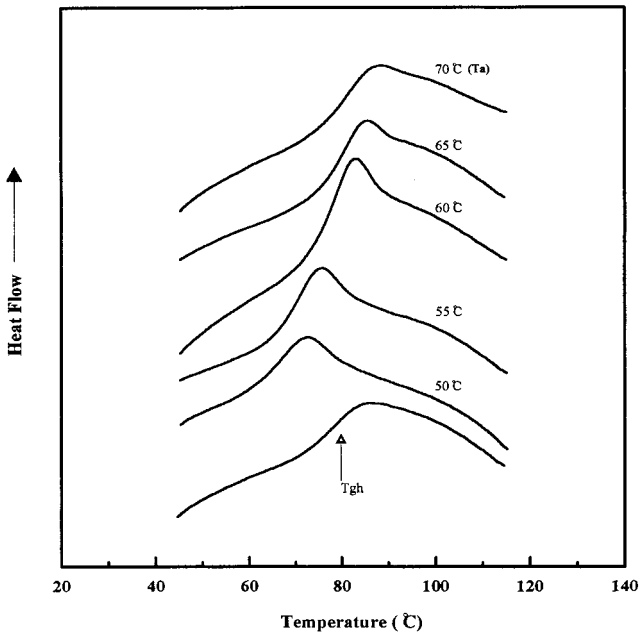

Figure 6. DSC thermograms for the melt-quenched PU2300-69 samples, which were further annealed under different annealing temperature, T_a, for 1 h.

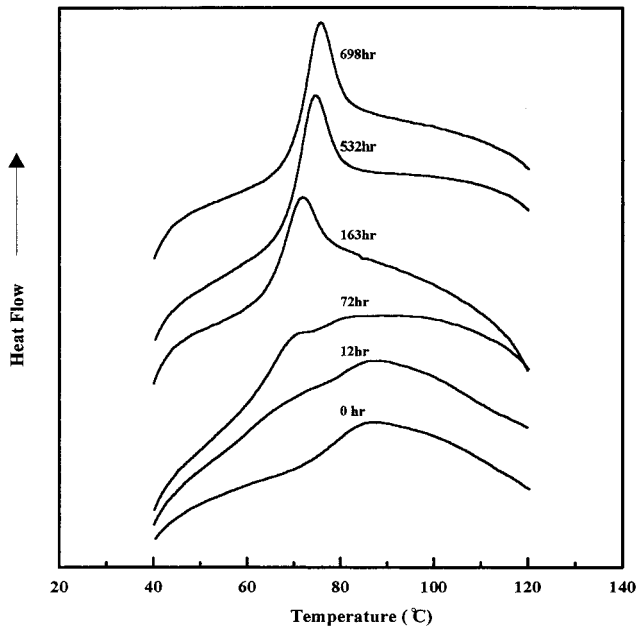

Figure 7. Enthalpy relaxation behaviors of the melt-quenched PU2300-69 samples, which were further annealed under different physical aging time at 30 °C.

must also retain its complete phase separation up to 230 °C, accordingly.

The discussion of complete phase separation for the samples, below and above the hard-segment glass transition temperature, is important in that we can first assume that T_1 behavior would not relate to the soft-segment phase and the hard/soft-segment dissolution. Thus, the proposed T_1 nature originating from the hard-segment dissolution[7] may be excluded at the present study.

The clear location of hard-segment glass transition temperature is also important in that it allow us to establish the relationship between T_1 and the T_{gh} of an amorphous hard-segment phase.

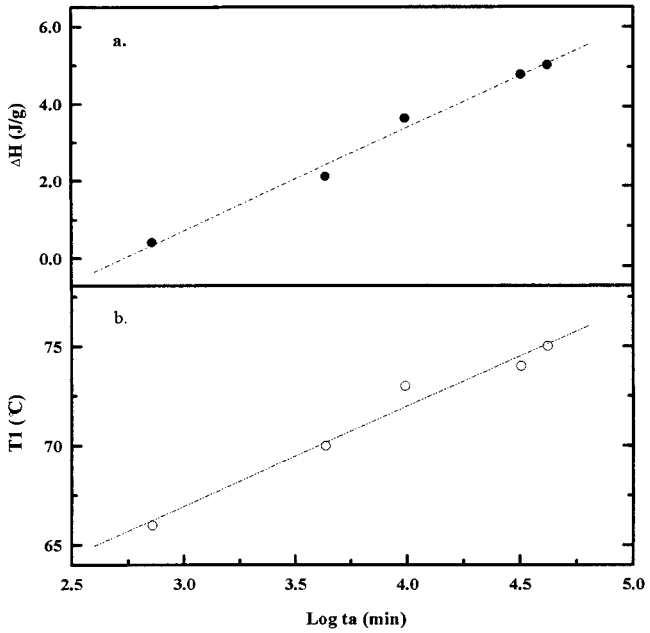

Figure 8. (a) Relationship of the excess enthalpy relaxation, ΔH, with respect to the logarithm of annealing time. (b) Relationship of the endothermic peak position, T_1, with respect to the logarithm of annealing time, t_a. Both a and b are results from DSC thermograms in Figure 7.

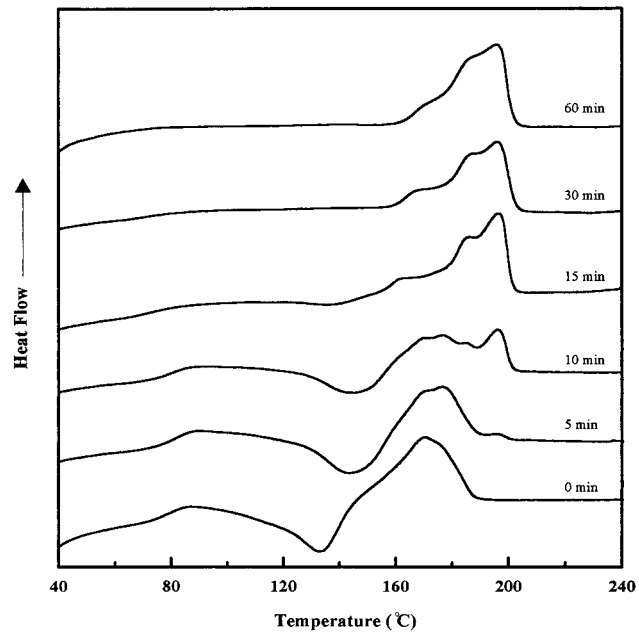

Figure 9. DSC thermograms for the melt-quenched samples of PU2300-69, which were further annealed at 150 °C for different time periods.

Since the literature T_1 values mostly appeared at above room temperature, the following DSC thermograms of the melt-quenched samples were only measured from the room temperature. All the samples indicated in the following sections refer to the melt-quenched samples, if there is no further description.

Effect of Sub-T_{gh} Annealing. Figure 4 shows the DSC thermograms of the melt-quenched PU2300-69 samples after further annealing at 60 °C for different time period. It is found that a small endotherm appearing in the vicinity of the hard-segment glass transition temperature progressively shifts to a higher temperature and grows larger in its magnitude as the

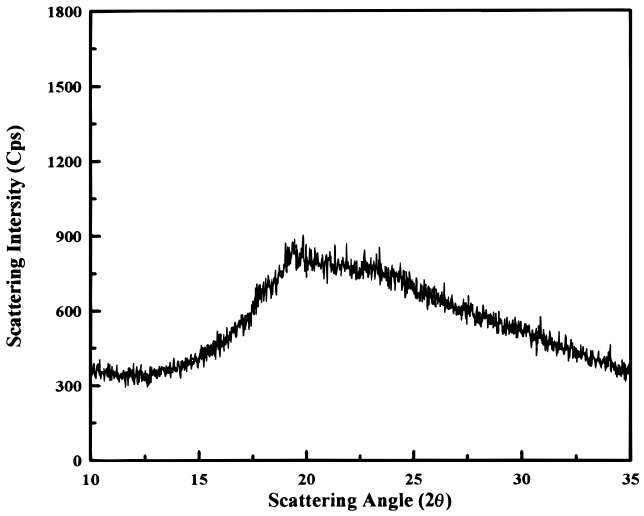

Figure 10. Wide-angle X-ray scattering profile of the melt-quenched PU2300-69 sample after further annealing at 150 °C for 1 h.

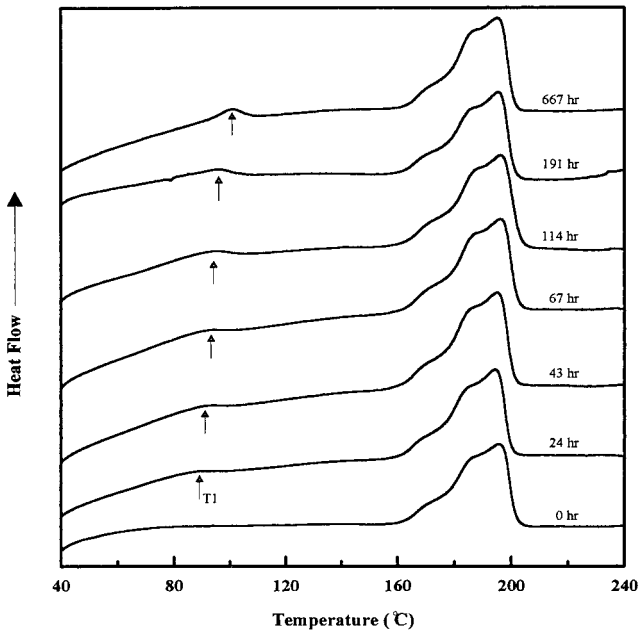

Figure 11. DSC thermograms for the melt-quenched PU2300-69 samples, which were further annealed at 150 °C for 1 h and then quenched to 60 °C for physical aging of different time period.

annealing time (t_a) increases. Parts a and b of Figure 5 show that there are linear relationships for the endotherm's magnitude (ΔH) and the position (T_1; by following the literature designations), respectively, with respect to the logarithm of annealing time (log t_a). Furthermore, Figure 6 shows the results of the melt-quenched PU2300-69 samples which were further annealed under different annealing temperatures (T_a) for 1 h. It can be found that the greatest endothermic behavior appears at $T_a \approx T_{gh} - 20$ °C.

On the basis of Figure 4 through Figure 6, we would like to compare these hard segments' T_1 behaviors with a well-known enthalpy relaxation behavior resulting from the physical aging of an amorphous homopolymer. The origin of physical aging phenomenon[19,20] was that it was not generally in the thermodynamic equilibrium when a polymer material was cooled at a finite rate through the T_g. The observed aging behavior was, in

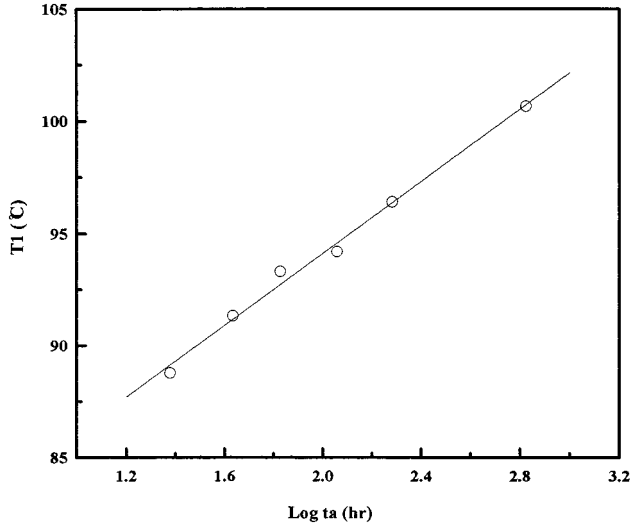

Figure 12. Relationship for the endothermic peak position, T_1, and the log t_a obtained from the DSC thermograms in Figure 11.

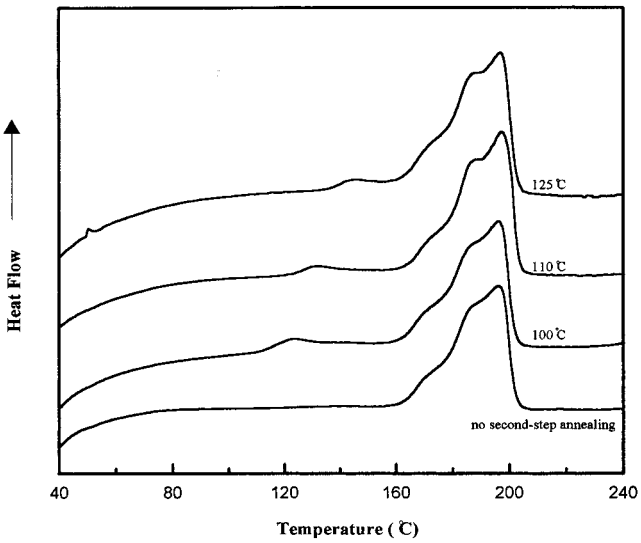

Figure 13. DSC thermograms for the melt-quenched PU2300-69 samples, which were further annealed at 150 °C for 1 h and then quenched to 100, 110, and 125 °C, respectively, for another 1-h annealing.

fact, due to the inherent nonequilibrium nature of the glassy state. During the cooling process the molecules were not able to reach their equilibrium conformation with respect to temperature due to the rapid increase in viscosity and the associated decrease in molecular mobility as the T_g was approached. There was thus a thermodynamic potential for the molecules to approach the equilibrium state by undergoing further packing and conformational changes. The molecular mobility below the T_g, although greatly reduced, remained finite, thus allowing the polymer molecules to approach the equilibrium state corresponding to a normal liquidlike packing. The measurable thermodynamic state functions, enthalpy and volume, had been found to decrease with increasing sub-T_g annealing time for pure amorphous glassy polymer. Tenbrinke et al. in their article[21] reviewed all the enthalpy relaxation behaviors from the physical aging of amorphous polymers and summarized the results as follows:

1. The magnitude of the endothermic peak at the proximity of T_g increases linearly with the logarithm of

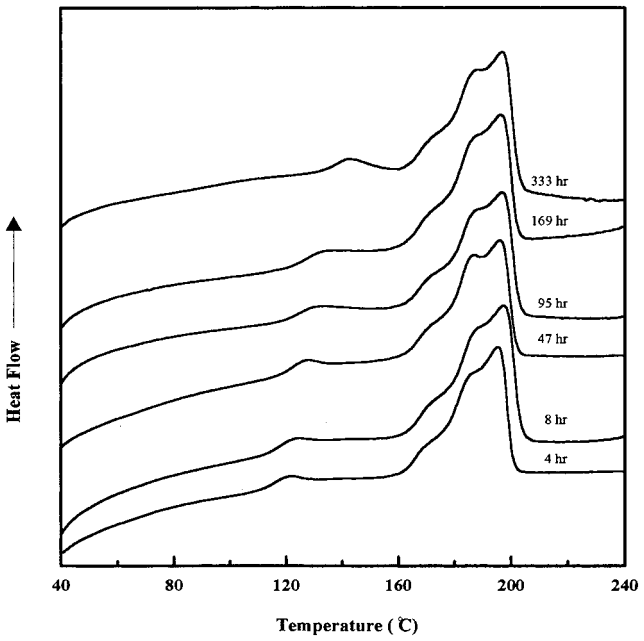

Figure 14. DSC thermograms of the melt-quenched PU2300-69 samples. The samples were further annealed at 150 °C for 1 h and, then, were annealed again at 100 °C for different time period.

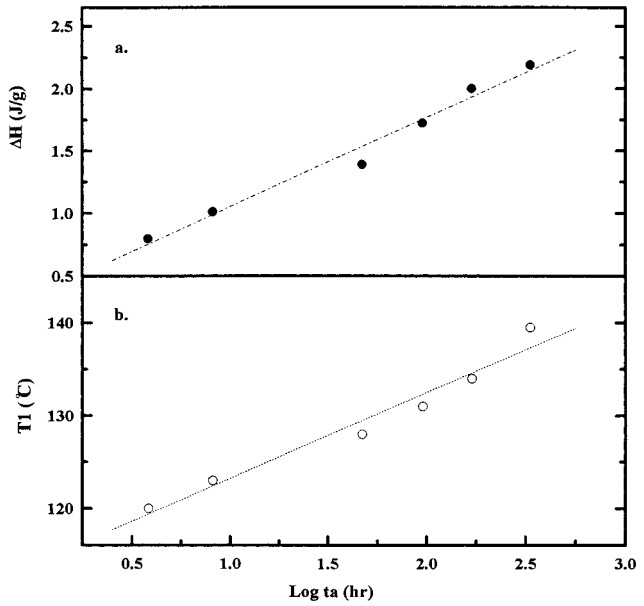

Figure 15. (a) Relationship of the excess enthalpy relaxation, ΔH, with respect to the logarithm of annealing time. (b) Relationship of the peak position, T_1, with respect to the logarithm of annealing time, Both a and b are results from DSC thermograms in Figure 14.

the annealing time (t_a), when the aged glass is not too close to equilibrium.[12−14,22−24]

2. The position of the endothermic peak also increases linearly with log t_a under the same conditions.[12,22,25−27]

3. The endothermic peak height passes through a maximum as a function of annealing temperature when $T_a = T_g - 20$ °C.[22,28]

In comparison to these enthalpy relaxation behaviors, it may be reasonable to assume that our polyurethane's endothermic behavior (T_1) from sub-T_{gh} annealing is an enthalpy relaxation behavior originating from the physical aging of an amorphous polyurethane hard segment.

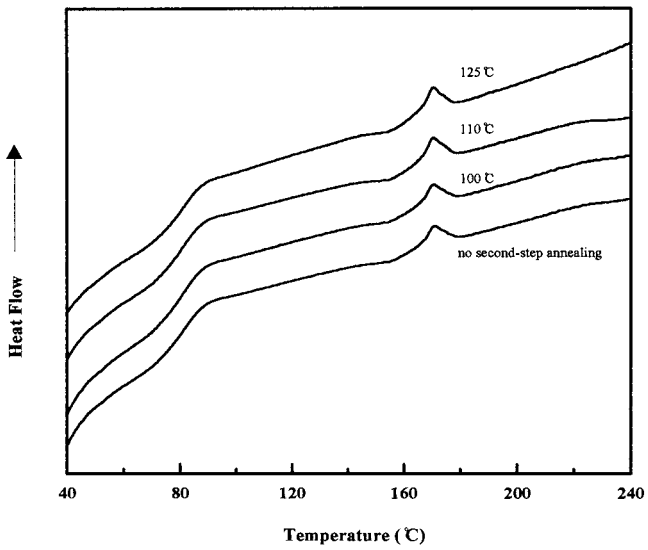

Figure 16. DSC thermograms for the melt-quenched PU1650-69 samples, which were further annealed at 175 °C for 1 h and, then, annealed again at 100, 110, and 125 °C, respectively, for another hour.

In the literature, Cooper et al.[2,3] proposed that the low-temperature endotherm (T_1) resulting from the room-temperature annealing of a polyurethane sample was a result of a destruction of the hard segment's short-range order. To further compare his conclusion, the melt-quenched PU2300-69 samples were further annealed at 30 °C for extended period of time. The DSC thermograms are shown in Figure 7. The position and the magnitude of the endothermic peak also increase linearly with the logarithm of the annealing time (Figure 8a,b). These results indicate that Cooper's previous short-range-order endotherm was probably an enthalpy relaxation resulting from prolonged physical aging at room temperature.

Although the polyurethane owns a soft microphase due to *cis*-polybutadiene segments, the main process of enthalpy relaxation could only develop in the amorphous hard-segment phase. This is because the present annealing temperature is much higher than that of the amorphous soft-segment T_g at around −110 °C and that of the soft segment T_m at around −20 °C.

Figure 3 indicates that for the PU2300-69 sample a reordering exotherm is terminated at 150 °C. If we have the sample annealed at this temperature, an ordered structure may be formed above this temperature. It would be interesting to study the enthalpy relaxation behavior from a sample with such a material structure. Thus, samples of the melt-quenched PU2300-69's were further annealed at 150 °C for different time periods (Figure 9). As the annealing time increases, the heat capacity change (ΔC_{ph}) at the hard-segment glass transition decreases and the magnitudes of three endotherms which appear between 160 °C and 200 °C increase. According to the previous polyurethane literature, endotherms appearing within this temperature range are associated with a noncrystalline long-range order of an unspecified nature (designated as T_2).[1−5,7,29] Multiple T_2's were frequently encountered in the literature.[4,29] However, the first peak appears at 170 °C, which is just 20 °C above the annealing temperature, is probably an enthalpy relaxation resulting from the physical aging (annealing) at 150 °C. The simultaneous decrease ΔC_p of the ΔC_{ph} and the increase of the

magnitude of the multiple endotherms seems to indicate that most of the amorphous glassy hard segment material has been changed into a noncrystalline T_2 material. Our WAXS study does show an almost complete amorphous halo (Figure 10) for this material.

Figure 9 also indicates that the T_2 structures can be fully developed after 1 h at 150 °C. Thus, after 1 h annealing at 150 °C, the PU2300-69 samples were quenched to 60 °C for further sub-T_{gh} annealing. Their endothermic behaviors after different annealing time are shown in Figure 11. The magnitude of the T_1 endotherm is very small and is hardly measurable. However, its position is still clearly shown. It is interesting to note that a linearly relationship between the position of the T_1 endotherm and log t_a is also found in Figure 12. This indicates that this new type of T_1 may also be an enthalpy relaxation appearing in this strong T_2 material.

Effect of Super-T_{gh} Annealing. It has always been indicated that an enthalpy relaxation would be expected from sub-T_g annealing assuming there is enough noncrystalline polymer present. From the above study, a noncrystalline T_2 material seems to give rise to a much reduced enthalpy relaxation behavior at a particular sub-T_{gh} temperature. To know how T_2 affects the enthalpy relaxation behavior, it would be worthwhile to study the effect of super-T_{gh} annealing on this strong T_2 material. Again, the melt-quenched PU2300-69 samples were preconditioned at 150 °C for 1 h in order to form the T_2 structures for the hard-segment phase. These samples were then quickly quenched to 100, 110, and 125 °C, respectively, for a second-step 1-h super-T_{gh} annealing. After these thermal treatment, the DSC thermograms are shown in Figure 13. The multiple endotherms appearing between 160 and 200 °C are the so-called long-range order structures resulting from the annealing at 150 °C. The total enthalpy of the multiple endotherms equals 34.16 ± 0.51 J/g. The small endotherms appearing at 120, 131, and 145 °C may be due to the enthalpy relaxation resulting from the 100, 110, and 125 °C annealing, respectively, since the position of these endotherms, designated as T_1's, increases with the increase of annealing temperature, and the relationship of $T_1 - T_a \approx 20$ °C also holds for these super-T_{gh} annealings. On the other hand, if the preconditioned (150 °C/1 h) PU2300-69 samples were further annealed at 100 °C for different time periods, the position and magnitude of the endotherms progressively increase with the increase of annealing time (Figure 14). Parts a and b of Figure 15 also show the linear relationships of the position and the magnitude, respectively, with the logarithm of annealing time, log t_a. In summary, all the T_1 behaviors in Figures 13 and 14 are typical of the enthalpy relaxation. However, the T_1 magnitudes (ΔH) are much smaller than those expected for a highly amorphous hard-segment phase. Also, the T_1 positions can appear in a very wide range of super-T_{gh} temperatures and can shift to a temperature near the vicinity of T_2 endotherms. From these results and from the generally accepted concept that enthalpy relaxation can only appear in a temperature below the amorphous glass transition temperature, we propose that this preformed T_2 structure may disturb the amorphous hard phase, reduce the segmental mobility, and shift the hard segment T_g in different degrees to a temperature near the vicinity of the T_2 endotherms. This proposal may provide good explanation for the T_1 behaviors in Figures 13 and 14 and, on the other hand, may add to the understanding of the long-term confusing nature of the T_2 structure.

On the basis of the general concept of an enthalpy relaxation, a pure amorphous polymer should not exhibit enthalpy relaxation while annealed at above its glass transition temperature. Our final study would display this fact. Samples of the melt-quenched PU1650-69 ($T_{gh} \approx 80$ °C) were first preconditioned at 175 °C for 1 h and then quenched to room temperature for another DSC scanning. The DSC scanning under this condition is presented at the lowest thermogram in Figure 16. The DSC baselines before and after the glass transition temperature are quite level. However, there is still a very small endotherm appearing at 175 °C. An endotherm appearing at this temperature has been previously considered as indicating the destruction of a long-range order (T_2) formed during quenching. However, the T_2 enthalpy here is very small (1.2 J/g). It is only 3.5% when compared with the total magnitude of the multiple T_2 endotherm (34.16 J/g) of the PU2300-69 sample in Figure 13, indicating that only a negligible amount of the T_2 structure was found for the preconditioned PU1650-69 sample. Three other preconditioned PU1650-69 samples were then quenched to 100, 110, and 125 °C, respectively, for a second-step 1-h annealing. These DSC thermograms are also shown in Figure 16. There are no endotherms occurring at temperature higher than the respective annealing temperatures except the preexisting T_2. This indicates that without enough coexisting T_2 structure, the amorphous hard segment cannot exhibit an enthalpy relaxation at a temperature above its T_g.

The assumption that there is a complete phase separation for PU1650-69 sample can be further confirmed by this Figure 16, since all the baselines before and after T_{gh}, are quite level and all the T_{gh}'s and ΔC_p's are basically equivalent after the samples were thoroughly annealed at 100, 110, and 125 °C, respectively, for 1 h. These indicate that there was no difference in the hard/soft segment dissolution after different high-temperature annealings. Only a highly phase-separated system can make this possible. On the other hand, since PU2300-69 samples have both higher soft-segment and higher hard-segment molecular weights than PU1650-69, it would be a complete phase-separated system, accordingly.

In segment polyurethanes, the mechanical properties were generally accredited to the result of a pseudo-cross-linking effect[30] resulting from the hard-segment aggregation. The hard-segment domain generally exhibits a different degree of order or semicrystalline structure which was considered to be able to reinforce the hard-segment domain. Nevertheless, the amorphous region has never been studied in the literature. However, the presence of an amorphous material may constitute the weakest part inside the hard-segment domain. Catastrophic failure of the pseudo-cross-linking may start from this region. Since physical aging would densify and strengthen the hard-segment domain from the weakest point, the mechanical properties of the polyurethane may be improved by a proper control of the physical aging. In addition, the rise of hard-segment T_g from the formation of T_2 structure would also strengthen the hard phase domain and lead to an enhanced mechanical property. Thus, this present study may provide two possibilities to enhance the

mechanical property of the polyurethane material. Our preliminary results do show great enhancements.[31] It will be presented in a separate paper.

Conclusions

A series of segment polyurethanes based on MDI and BD as the hard segment and *cis*-polybutadiene as the soft segment were synthesized. Some of these polyurethanes have been found to be completely phase-separated even at a temperature well above their hard-segment glass transition temperature. These complete phase-separated polyurethanes were used for the study of the long-term confusing short-range-order endotherm (T_1) by differential scanning calorimetry. Evidence for complete phase separation would exclude the possibility of T_1 formation in relation to the soft-segment phase and to the hard/soft segment dissolution. A highly amorphous hard-segment phase and a clear hard-segment glass transition temperature were found for the melt-quenched PU1650-69 and PU2300-69 samples. These glass transition behavior are important in two aspects. First, substantial hard phase heat capacity changes, ΔC_{ph}, were found for the samples, indicating that the literature assumption[4,32] of $\Delta C_{ph} = 0$ for the polyurethane hard segment is incorrect. Details on the study of the pure hard-segment glass transition behavior will be presented in a separate paper. Second, the clear amorphous hard-segment T_g values enable us to study the T_1 behavior in relation to it. This is the main concern in this study. After extensive annealing studies on the samples with a highly amorphous hard-segment phase and the samples with preformed T_2 structures in the hard-segment phase and on the annealing temperature below the pure amorphous hard-segment T_g and above the pure amorphous hard-segment T_g, we suggest that the T_1 endotherm is an enthalpy relaxation behavior resulting from a prolonged physical aging process. On the other hand, we also suggest that the T_2 structure would reduce the hard-segment mobility and raise the hard-segment T_g in different degrees to a temperature near the vicinity of T_2.

Since the amorphous hard-segment region is the weakest part of the polyurethane hard phase, densifing the amorphous hard-segment region by proper physical aging and/or raising the T_g by the formation of a T_2 structure would, therefore, greatly reinforce the hard phase integrity and, thus, greatly improve the mechanical properties of the polyurethane materials. This study may, thus, point out two possible routes to further improve the mechanical properties of this important industrial polymer.

References and Notes

(1) Seymour, R. W.; Cooper, S. L. *Macromolecules* **1973**, *6*, 48.
(2) Hesketh, T. P.; Van Bogart, J. W. C.; Cooper, S. L. *Polym. Eng. Sci.* **1980**, *20*, 190.
(3) Van Bogart, J. W. C.; Bluemke, D. A.; Cooper, S. L. *Polymer* **1981**, *22*, 1428.
(4) Leung, L. M.; Koberstein, J. T. *Macromolecules* **1986**, *19*, 706.
(5) Koberstein, J. T.; Russell, T. P. *Macromolecules* **1986**, *19*, 714.
(6) Koberstein, J. T.; Galambos, A. F.; Leung, L. M. *Macromolecules* **1992**, *25*, 6195.
(7) Hu, W.; Koberstein, J. T. *J. Polym. Sci., Polym. Phys. Ed.* **1994**, *32*, 437.
(8) Kwei, T. K. *J. Appl. Polym. Sci.* **1982**, *27*, 2891.
(9) Koberstein, J. T.; Stein, R. S. *J. Polym. Sci., Polym. Phys. Ed.* **1983**, *21*, 1439.
(10) Chen, T. K.; Chui, J. Y.; Shieh, T. S. *Macromolecules* **1997**, *30*, 5068.
(11) Chen, T. K.; Hwung, C. J. *Proc. 10th ROC Polym. Symp.* **1987**, 790.
(12) Richardson, M. J.; Savill, N. G. *Polymer* **1977**, *18*, 413.
(13) Ellis, T. S. *Macromolecules* **1990**, *23*, 1494.
(14) Agrawal, A. *J. Polym Sci., Polym. Phys. Ed.* **1989**, *27*, 1449.
(15) Bengtson, B.; Feger, C.; Macknight, W. J.; Schneider, N. S. *Polymer* **1985**, *26*, 895.
(16) Speckhard, T. A.; Gibson, P. E.; Cooper, S. L.; Chang, V. S. C.; Kennedy, J. P. *Polymer* **1985**, *26*, 55.
(17) Chen, T. K.; Chui, J. Y.; Shieh, T. S. Submitted for publication.
(18) Chen, T. K.; Shieh, T. S. Manuscript in preparation.
(19) Struik, L. C. E. *Physical Aging in Amorphous Polymers and Other Materials*; Elsevier: Amsterdam, 1978.
(20) Hutchinson, J. M. *Prog. Polym. Sci.* **1995**, *20*, 703.
(21) Tenbrinke, G.; Grooten, R. *Colloid Polym. Sci.* **1989**, *267*, 992.
(22) Hodge, I. M.; Berens, A. R. *Macromolecules* **1982**, *15*, 762.
(23) Shen, J.; Shao, Z.; Li, S. *Polymer* **1995**, *36*, 3479.
(24) Hourston, D. J.; Song, M.; Hammiche, A.; Pollock, H. M.; Reading, M. *Polymer* **1996**, *37*, 243.
(25) Berens, A. R.; Hodge, I. M. *Macromolecules* **1982**, *15*, 756.
(26) Bosma, M.; ten Brinke, G.; Ellis, T. S. *Macromolecules* **1988**, *21*, 1465.
(27) McGowan, C. B.; Kim, D. Y.; Blumstein, R. B. *Macromolecules* **1992**, *25*, 4568.
(28) Hodge, I. M. *Macromolecules* **1983**, *16*, 898.
(29) Galambos, A. F.; Koberstein, J. T. *Polym. Mater. Sci. Eng.* **1989**, *61*, 359.
(30) Speckhard, T. A.; Cooper, S. L. *Rubber Chem. Technol.* **1986**, *59*, 405.
(31) Chiou, Y. T. M.S. Thesis, National Central University, Chungli, Taiwan, 1996.
(32) Koberstein, J. T.; Leung, L. M. *Macromolecules* **1992**, *25*, 6205.
(33) Petrovic, Z. S.; Budinski-Simendic, J. *Rubber Chem. Technol.* **1985**, *58*, 685.

MA970913M